International Journal of Mass Spectrometry 436 (2019) 71–78

Contents lists available at ScienceDirect

International Journal of Mass Spectrometry

journal homepage: www.elsevier.com/locate/ijms

Full Length Article

Gas phase fragmentation of adducts between dioxygen and *closo*-borate radical anions

Jonas Warneke [a,*], Markus Rohdenburg [b], Judy K.Y. Liu [a], Erynn Johnson [a], Xin Ma [a], Rashmi Kumar [a], Pei Su [a], Edoardo Aprà [c], Xue-Bin Wang [d], Carsten Jenne [e], Maik Finze [f], Hilkka I. Kenttämaa [a], Julia Laskin [a,*]

[a] *Department of Chemistry, Purdue University, West Lafayette, 560 Oval Drive, IN, 47907, USA*
[b] *Institute for Applied and Physical Chemistry, Faculty 2-Biology/Chemistry, Leobener Str. 5 (NW2), 28359 Bremen, Germany*
[c] *Environmental Molecular Sciences Laboratory, Pacific Northwest National Laboratory, 902 Battelle Boulevard, P. O. Box 999, Richland, WA, 99352, USA*
[d] *Physical Sciences Division, Pacific Northwest National Laboratory, 902 Battelle Boulevard, P.O. Box 999, MSIN K8-88, WA, 99352, USA*
[e] *Anorganische Chemie, Fakultät für Mathematik und Naturwissenschaften, Bergische Universität Wuppertal, Gaußstr. 20, 42119 Wuppertal, Germany*
[f] *Julius-Maximilians-Universität Würzburg, Institute for Inorganic Chemistry, Institute for Sustainable Chemistry & Catalysis with Boron (ICB), Am Hubland, 97074 Würzburg, Germany*

ARTICLE INFO

Article history:
Received 27 July 2018
Received in revised form 22 October 2018
Accepted 1 November 2018
Available online 12 November 2018

Keywords:
Closo-borate anions
Radical anion chemistry
Dioxygen addition
Collision induced dissociation
Photoelectron spectroscopy

ABSTRACT

The icosahedral *closo*-borate anions, $[closo\text{-}B_{12}X_{12}]^{2-}$ (B_{12}) and $[1\text{-}H\text{-}closo\text{-}1\text{-}CB_{11}X_{11}]^{-}$ (CB_{11}) with X=H or halogen, are exceptionally stable weakly coordinating anions. Recent studies, which focused on the gas phase ion chemistry of this class of anions, revealed several unusual ion-molecule and unimolecular dissociation pathways. Herein, we demonstrate that collisional activation of highly iodinated *closo*-borate anions results in a loss of an iodine atom followed by a spontaneous addition of O_2 present in a mass spectrometer background producing B_{12}-O_2 and CB_{11}-O_2 species. We examined the electronic structure of a representative O_2 adduct using photoelectron spectroscopy and explored collision-induced dissociation (CID) pathways of a series of iodinated B_{12}-O_2 and CB_{11}-O_2 anions with different substituents. A systematic study of the gas phase dissociation pathways of the B_{12}-O_2 and CB_{11}-O_2 anions revealed several unusual dissociation pathways characteristic of this class of species. Abundant fragment ions are formed by neutral loss of $BOX_2^{\bullet}$ (X = boron bound substituent), $Y_2H^{\bullet}$ (Y = boron bound halogen, if any H is present in the molecular ion) and $BO_2^{\bullet}$. Loss of $BO_2^{\bullet}$ was observed for CB_{11}-O_2 but not for B_{12}-O_2 anions. Substantial differences in stability of the corresponding fragments are responsible for the observed differences in dissociation of B_{12}-O_2 and CB_{11}-O_2 species. Furthermore, we show that in addition to O_2 other molecules with a radical character (e.g. $SCH_3^{\bullet}$) can form adducts with *closo*-borate anions after iodine abstraction. The boron cage fragmentation observed for the O_2 adducts is atypical for highly iodinated *closo*-borates and is attributed to the strength of B—O bonds which dominate the thermochemistry of B_{12}-O_2 and CB_{11}-O_2 fragmentation reactions.

1. Introduction

In the condensed phase and in the gas phase, the chemistry of carbon is much better understood than the chemistry of boron, its neighbor in the periodic table of elements. Although organic-like compounds can be generated through the formation of boron-boron single bonds [1], boron is better known for a variety of polyhedral compounds classified by the Wade rules. [2,3] Three-center-two-electron (3c2e) bonds are the characteristic bonding motif of polyhedral boron compounds. Understanding the molecular properties of these compounds is of high relevance to medical applications, e.g. boron neutron capture therapy of cancer or inhibition of the HIV protease. [4] The best explored polyhedral boron compounds are the *closo*-dodecaborate ions with the general formula $[closo\text{-}B_{12}X_{12}]^{2-}$ (Fig. 1a; in the following abbreviated as B_{12}). In these species, each boron atom is bound to one *exo*-substituent, X, by a common 2c2e bond and is incorporated into a delocalized σ-electron system within the icosahedral $\{closo\text{-}B_{12}\}$ moiety. This exceptional structural motif stabilizes two excess electrons in a small molecular framework. Therefore, *closo*-dodecaborate anions attracted attention within the field of small multiply charged anions (MCAs) for many years [5,6] and recent theoretical investigations predict derivatives of this compound

* Corresponding authors.
E-mail addresses: jwarneke@purdue.edu (J. Warneke), jlaskin@purdue.edu (J. Laskin).

https://doi.org/10.1016/j.ijms.2018.11.005
1387-3806/

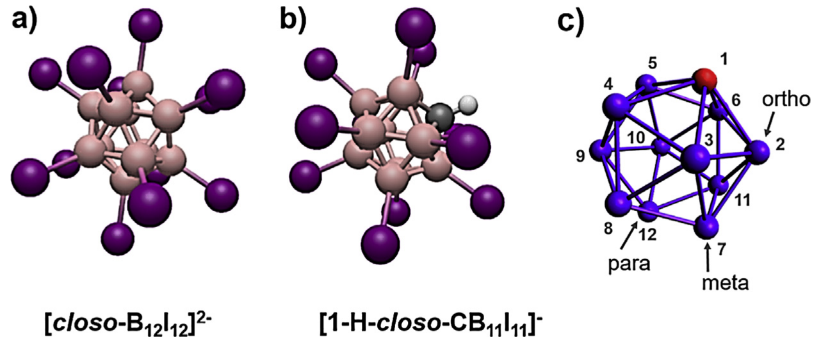

Fig. 1. Structures of a) the periodinated *closo*-dodecaborate dianion (B_{12}) and b) the undecaiodinated carba-*closo*-dodecaborate anion (CB_{11}, B - pink, I - purple, C - grey, H - white); c) Nomenclature for carbon and boron atoms in the CB11 ions (substituents not shown), position 1 is assigned to the carbon atom (marked in red). Positions relative to the carbon atom are referred to as *ortho*, *meta* or *para*, respectively.

class to be the most electronically stable MCAs known today [7,8]. Exchange of one B-X unit by a C-H unit results in the singly charged carba-*closo*-dodecaborate anions [1-H-*closo*-1-$CB_{11}X_{11}$]$^-$ (in the following abbreviated CB_{11}), see Fig. 1b. The halogenated versions (X = halogen) of these icosahedral B_{12} and CB_{11} ions are used as very inert weakly coordinating anions [9] to stabilize highly reactive cations in chemical synthesis [10,11] and catalysis [12].

To understand the molecular properties of *closo*-dodecaborate anions including their electronic structure and reactivity, we are exploring these ions in the gas phase. The electronic properties of [*closo*-$B_{12}X_{12}$]$^{2-}$ (X = F,Cl,Br,I) have been examined using gas-phase photoelectron spectroscopy (PES) and theoretical investigations. [13] Furthermore, we investigated the acidity of H[$B_{12}X_{12}$]$^-$ ions [14] and host-guest chemistry [15] of [*closo*-$B_{12}X_{12}$]$^{2-}$ ions with organic host-molecules in the gas phase. Interactions of [*closo*-$B_{12}F_{12}$]$^{2-}$ with metal cations [16] and with $C_6H_6F_6$, which has an unusually strong dipole moment have been examined by Hopkins and coworkers [17]. Contrary to their exceptional inertness in the condensed phase, collision-induced dissociation (CID) of halogenated B_{12} ions provides access to a large number of fragment ions with an unusual reactivity in the gas phase. [18] Structural transformations of the {*closo*-$B_{12}X_n$} species obtained by stripping off the ligands were characterized using gas-phase infrared (IR) spectroscopy and molecular modeling [19,20]. An exceptional reactivity was observed for [*closo*-$B_{12}X_{11}$]$^-$ anions produced in the first fragmentation step of [*closo*-$B_{12}X_{12}$]$^{2-}$ (X = Cl,Br,I). In particular, it has been demonstrated that the free boron atom in the singly charged [*closo*-$B_{12}X_{11}$]$^-$ anionic fragment is highly electrophilic. [21] This electrophilic site promotes the spontaneous binding of water and dinitrogen from the residual background gas in a mass spectrometer. Moreover, binding of krypton and xenon at room temperature was demonstrated with [*closo*-$B_{12}Cl_{11}$]$^-$ [21]. For X = Cl,Br, halide ion loss is the only dominant primary fragmentation channel. In contrast, [*closo*-$B_{12}I_{12}$]$^{2-}$ shows the competing loss of an iodine radical. The homolytic bond cleavage produces a radical dianion, [*closo*-$B_{12}I_{11}$]$^{2-\bullet}$, which spontaneously adds an O_2 molecule - a previously unreported adduct formation of *closo*-borate ions. In this study we explore the gas phase ion chemistry of such unusual radical anions: [*closo*-$B_{12}X_{11}(O_2)$]$^{2-\bullet}$ and the related [1-H-*closo*-1-$CB_{11}X_{10}(O_2)$]$^{-\bullet}$ species. CID of these dioxygen adducts leads to previously unknown chemical transformations of the *closo*-borate scaffolds described in this study.

2. Methods

2.1. Mass spectrometry

2.1.1. Ion molecule reactions with O_2

Salts containing the investigated *closo*-borate anions and different alkylated ammonium counterions were dissolved in methanol to concentrations of roughly 10^{-6} mol/L and the solutions were injected using a syringe pump into the inlet of a Bruker Esquire LC Ion Trap (Bruker Daltonics, Bremen) or a Thermo LTQ XL (Thermo Scientific) ion trap mass spectrometer with flow rates of roughly 3 μL/min. The analytes were ionized using electrospray ionization (ESI). CID experiments were performed using helium as collision gas. Ions with a specific *m/z* value were isolated with a window of ten *m/z* units (based on the broad isotopic patterns of B_{12} and CB_{11} ions) and activated by applying an adjustable ac voltage to the ion trap end caps. The radical anions, which react with dioxygen, were stored in the ion trap for 1–3 seconds. The O_2 adducts were subsequently isolated and activated.

2.1.2. Ion-molecule reaction with dimethyl disulfide

The *closo*-borate anion solution was delivered at a flow rate of 10 μL/min using a syringe pump and ionized by electrospray ionization at the inlet of a Thermo LTQ linear quadrupole ion trap mass spectrometer (Thermo Scientific). A home-built reagent mixing manifold was used to introduce the reagent vapor, dimethyl disulfide (DMDS) purchased from Sigma Aldrich, directly into the ion trap. DMDS was injected at a flow rate of 5 μL/h, vaporized and mixed with the constant helium flow as the carrier gas. The borate anion was subjected to in-source CID (collision energy 80 V) to generate the radical dianion, and the radical dianion was allowed to react with DMDS in the ion trap for a variable reaction time ranging from 10 to 100 ms. The reaction product ion was then isolated and subjected to CID to obtain structural information.

2.2. Photoelectron spectroscopy

Photoelectron Spectroscopy (PES) experiments were performed with an apparatus consisting of a custom-designed ESI source, a temperature-controlled cryogenic ion trap, and a magnetic-bottle time-of-flight (TOF) photoelectron spectrometer, as described elsewhere. [22] Acetonitrile solutions of *closo*-borate salts (0.1 mM) were used for electrospray. The ions generated by ESI were guided by quadrupole ion guides into the ion trap, where they were accumulated and cooled for 20–100 ms by collisions with a cold buffer gas (20% H_2 balanced in helium) at 20 K, before being transferred into the extraction zone of a TOF mass spectrometer. The cooling of the anions to 20 K improved spectral energy resolution and eliminated the possibility of the appearance of peaks in the PE spectra, due to hot bands. The anions were mass selected and decelerated prior to photodetachment with 157 nm photons (7.866 eV) from an F_2 excimer laser. The laser was operated at a 20 Hz repetition rate, with the ion beam off at alternating laser shots, affording shot-to-shot background subtraction. Photoelectrons were collected with ~100% efficiency using a magnetic bottle and analyzed in a 5.2 m long electron flight tube. The recorded PES spectrum was converted into an electron kinetic energy spectrum by calibration with the known photoelectron spectra of I^- [23] and $[OsCl_6]^{2-}$ [24]. The electron binding energy (EBE) was obtained by subtracting the electron kinetic energy from the energy of the detaching photons. The energy resolution was about 2%, i.e., ~20 meV for 1 eV kinetic energy electrons. Details about interpretation of PES spectra can be found in SI1.

2.3. Computational investigations

Computational studies were performed either with (a) the Gaussian09 software suite [25] employing the B3LYP/6-311++G(2d,2p) [26,27] model chemistry, except for iodine atoms, which were described by the same DFT hybrid functional but the Stuttgart-Dresden (SDD) basis set and pseudo potential or (b) the NWChem software [28] using B3LYP/def2-tzvppd [29]. We used the DFT-D3 dispersion correction [30] with the Becke-Johnson damping function (GD3BJ) in both cases. [31] Geometry optimizations were carried out and the obtained structures were confirmed to be minimum geometries by the absence of imaginary vibrational modes in subsequent frequency analyses. Open-shell radical species were computed using the unrestricted Kohn-Sham formalism for calculation of molecular orbitals, i.e. singly occupied orbitals for electrons of alpha and beta spin were not been constrained to be equal in energy. Reaction thermochemistry was calculated by subtracting the energy of the reactant from energies of reaction products both being corrected for Zero-Point vibrational Energies (ZPEs), i.e. 0 K reaction enthalpies were calculated. Both starting materials and reaction products were fully optimized.

2.4. Boron compounds

Salts of the ions $[closo\text{-}B_{12}I_{12}]^{2-}$ [32], $[closo\text{-}B_{12}I_{11}(NH_2)]^{2-}$ [33], $[1\text{-}H\text{-}closo\text{-}CB_{11}I_{11}]^-$ [34], $[1\text{-}H_2N\text{-}closo\text{-}CB_{11}I_{11}]^-$ [34] and $[1\text{-}H_2N\text{-}2\text{-}F\text{-}closo\text{-}CB_{11}I_{10}]^-$ [35] were synthesized according to known procedures. The ions $[closo\text{-}B_{12}I_{11}H]^{2-}$, $[closo\text{-}B_{12}I_{11}Cl]^{2-}$, $[closo\text{-}B_{12}I_{11}(OH)]^{2-}$ and $[closo\text{-}B_{12}I_{10}H_2]^{2-}$ were isolated in the ion trap from incomplete iodination reactions of $[closo\text{-}B_{12}H_{12}]^{2-}$. The anions $[1,2\text{-}H_2\text{-}closo\text{-}1\text{-}CB_{11}I_{10}]^-$ and $[1\text{-}H\text{-}closo\text{-}1\text{-}CB_{11}I_9H(OH)]^-$ were identified as minor components in iodination reactions of $[1\text{-}H\text{-}closo\text{-}1\text{-}CB_{11}H_{11}]^-$. The partially iodinated anions $[1\text{-}H_2N\text{-}2\text{-}F\text{-}closo\text{-}1\text{-}CB_{11}I_{10\text{-}n}H_n]^-$ (n = 1–3) were isolated from the crude product of the reaction mixture before full iodination. $[1\text{-}H\text{-}12\text{-}H_2N\text{-}closo\text{-}1\text{-}CB_{11}I_4H_4Cl_2]^-$ was obtained by reaction of $[1\text{-}H\text{-}12\text{-}H_2N\text{-}closo\text{-}1\text{-}CB_{11}H_{10}]^-$ with ICl [36] in a complex mixture with other mixed chlorinated and iodinated anions.

3. Results and discussion

In this study, we characterized structures, electronic properties, and gas phase fragmentation pathways of $[closo\text{-}B_{12}X_{11}(O_2)]^{2-\bullet}$ (B_{12}-O_2) and $[1\text{-}H\text{-}closo\text{-}CB_{11}X_{10}(O_2)]^{-\bullet}$ (CB_{11}-O_2) radical anions. These species are produced by the O_2 attachment to radical fragments originating from the loss of an iodine atom from $[closo\text{-}B_{12}X_{12}]^{2-}$ and $[1\text{-}H\text{-}closo\text{-}CB_{11}X_{11}]^-$, respectively. Although the reactivity of *closo*-borate fragment ions which originate from the halide ion loss (reaction path 1 in Fig. 2) was examined previously, ion molecule chemistry of these ions following the radical halogen loss (reaction path 2 in Fig. 2) has not been reported. Dioxygen addition was reported for some radical cations [37–39] but remains a rare phenomenon for anions [40]. This ion-molecule reaction provides access to interesting molecular ions that have not yet been characterized by mass spectrometry (*vide infra*).

The discussion of the anion characterization is divided into three sections. First, we describe the electronic structure of such adducts

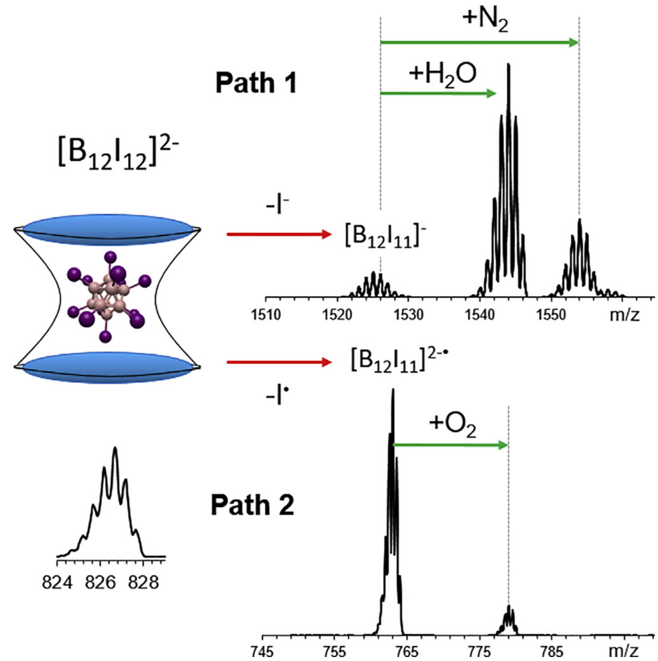

Fig. 2. Reaction pathways of $[closo\text{-}B_{12}I_{12}]^{2-}$ after isolation and CID. Red arrows indicate fragmentation reactions initiated by CID and green arrows indicate spontaneous addition reactions. Path 1 (even electron path) has been described in detail in a previous publication.[18] Reaction products of path 2 (radical path) are investigated here for the first time. In the isotopic pattern of B_{12} ions, the highest abundance peak contains ten ^{11}B and two ^{10}B isotopes.

using $[closo\text{-}B_{12}I_{11}(O_2)]^{2-\bullet}$ as a model system. Next, we examine the effect of substituents, X, on the fragmentation pathways of B_{12}-O_2 and CB_{11}-O_2 anions. Finally, we provide first insights into the possibility of substituting the O_2 moiety with other reactive gases and compare gas phase fragmentation of the resulting adducts.

3.1. Electronic structure of $[closo\text{-}B_{12}I_{11}(O_2)]^{2-\bullet}$

We investigated the electronic structure of $[closo\text{-}B_{12}I_{11}(O_2)]^{2-\bullet}$ experimentally using PES (Fig. 3a). A comparison with the PES spectrum of $[closo\text{-}B_{12}I_{12}]^{2-}$ shows strong similarities, confirming the integrity of the $\{closo\text{-}B_{12}\}$ structure after the O_2 attachment. The optimized molecular structure is shown in Fig. 3a. Calculation of the spin density revealed that in $[B_{12}I_{11}(O_2)]^{2-\bullet}$ the unpaired electron is mainly localized on the O_2 unit (Fig. 3b). The observed similarity between the first peak in the PES spectrum of $[closo\text{-}B_{12}I_{11}(O_2)]^{2-\bullet}$ at EBE = 2.84 eV and its even-electron counterpart, $[closo\text{-}B_{12}I_{12}]^{2-}$, at EBE = 2.80 eV indicates similar localization of the highest occupied molecular orbitals (HOMOs) in these systems. Computational investigations with different methods confirm that, in both anions, the HOMOs are localized predominantly on the iodine ligands (Fig. 3c) and are therefore separated from the formal radical site. Furthermore, in agreement with the experimental PES data, the calculated vertical detachment energies (VDEs) are very similar for both ions (details can be found in the supporting information). The high molecular symmetry of $[closo\text{-}B_{12}I_{12}]^{2-}$ (point group I_h, see structure in Fig. 1) results in degenerate orbitals and sharp, distinct signals in the PES spectrum (Fig. 3a). The bent O_2 substituent lowers the symmetry to point group C_s (structure in Fig. 3b), resulting in splitting in the energy levels of the electronic states, as confirmed by examining the calculated Hartree-Fock orbital energy levels shown in Fig. 3a below the PES spectra. This explains the general broadening or splitting of the spectral features in the PES spectrum of $[closo\text{-}B_{12}I_{11}(O_2)]^{2-\bullet}$ compared to $[closo\text{-}B_{12}I_{12}]^{2-}$ (Fig. 3a).

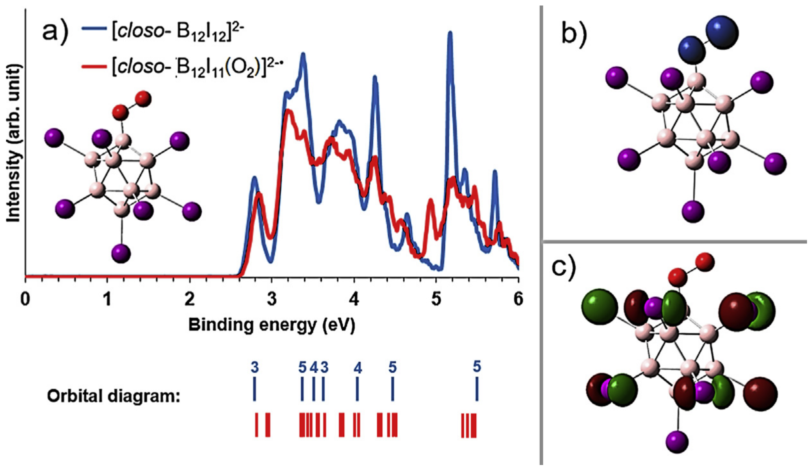

Fig. 3. a) Photoelectron spectra of [*closo*-$B_{12}I_{12}$]$^{2-}$ (blue) and [*closo*-$B_{12}I_{11}(O_2)$]$^{2-\bullet}$ (red) and optimized molecular structure of [*closo*-$B_{12}I_{11}(O_2)$]$^{2-\bullet}$ (B3LYP-GD3BJ/6-311++G(2d,2p)/SDD). Oxygens are shown in red. The energy levels of the Hartree Fock orbitals for both species are plotted below the PES spectra. Degenerate orbitals are labeled with a corresponding number. Note that the calculated HOMO energy was shifted to match the experimentally determined VDE according to the established procedure [41,42]. Comparison of the PES spectra confirms that both the geometry and electronic structure of [*closo*-$B_{12}I_{11}(O_2)$]$^{2-\bullet}$ are similar to [*closo*-$B_{12}I_{12}$]$^{2-}$. Note that the contribution of oxygen atomic orbitals to the Hartree-Fock orbitals is small. The first orbital with significant oxygen contribution is outside of the measurable range, b) spin density (blue, isovalue 0.005 a.u.). Additional information is provided in Figure S2; c) HOMO (orbital lobes in green and dark red, isovalue 0.04 a.u.) of [*closo*-$B_{12}I_{11}(O_2)$]$^{2-\bullet}$. Similar to [*closo*-$B_{12}I_{12}$]$^{2-}$, the HOMO in [*closo*-$B_{12}I_{11}(O_2)$]$^{2-\bullet}$ is delocalized across the iodine atoms. The spatial separation of HOMO and spin density was also confirmed using unrestricted Hartree-Fock calculations (UHF/def2-tzvppd). A detailed description of the computational investigations and the dependence of the HOMO-spin density separation predicted using different computational methods can be found in section SI1.

3.2. Collision-induced dissociation of B_{12} and CB_{11} ions with O_2 substituents

The CID spectrum of mass-selected [*closo*-$B_{12}I_{11}(O_2)$]$^{2-\bullet}$ is shown in Fig. 4a. The predominant fragment is [$B_{11}I_9O$]$^{2-}$, corresponding to a neutral loss of $BOI_2^{\bullet}$. This observation is remarkable, since boron-containing neutral losses have not been observed in CID experiments of [*closo*-$B_{12}I_{12}$]$^{2-}$ [18,19]. For comparison, we investigated a variety of B_{12}-O_2 and CB_{11}-O_2 ions, which contain both iodine and other ligands bound to boron. CID driven iodine loss from these precursors, followed by O_2 addition and subsequent fragmentation, gives access to unknown molecular ions generated from {*closo*-B_{12}} and {*closo*-CB_{11}} clusters, if different ligands are present. Fig. 4 shows representative CID spectra of the B_{12}-O_2 and CB_{11}-O_2 species formed from [*closo*-$B_{12}I_{12}$]$^{2-}$, [*closo*-$B_{12}I_{11}$(OH)]$^{2-}$, [1-H-*closo*-1-$CB_{11}I_{11}$]$^{-}$ and [1-D_2N-2-F-*closo*-1-$CB_{11}I_8H_2$]$^{-}$ precursor anions. Table 1 summarizes the results from all the investigated ions by listing the neutral losses which lead to the fragment ions observed in the spectra. Spectra not shown in Fig. 4 can be found in SI2. Different classes of neutral losses color-coded in Fig. 4 and Table 1 are discussed in detail below. We note that the molecular formulae of the neutral losses given below do not contain any structural information.

3.2.1. Loss of $BOX_2^{\bullet}$

$BOX_2^{\bullet}$ losses (red in Table 1) were common in the spectra of B_{12}-O_2 anions containing different boron-bound substituents, X. As discussed earlier, loss of $BOI_2^{\bullet}$ is the dominant fragmentation pathway observed for [*closo*-$B_{12}I_{11}(O_2)$]$^{2-\bullet}$ anion. Meanwhile, loss of $BOIH^{\bullet}$ is exclusively observed in the presence of boron-bound hydrogen atoms. In contrast, hydrogens of functional groups or hydrogens bound to the C atom of the {*closo*-1-CB_{11}} cluster do not contribute to this neutral loss (compare Fig. 4c and d). Although $BOF_2^{\bullet}$ has been identified spectroscopically, [43] molecules with a general formula $BOX_2^{\bullet}$ have received little attention in the past. Optimized structures of minima on the potential surface of possible $BOI_2^{\bullet}$ isomers are shown in SI3. Since neutral fragments cannot be detected in our experiments, we cannot unambiguously determine whether $BOX_2^{\bullet}$ loss is a one- or multistep process. However, we observed a low-abundance signal corresponding to the loss of $I^{\bullet}$ from [*closo*-$B_{12}I_{11}(O_2)$]$^{2-\bullet}$. Isolation and fragmentation of the formed [$B_{12}I_{10}O_2$]$^{2-}$ results in the loss of BOI, (see SI3) indicating that the neutral loss of $BOX_2^{\bullet}$ is likely a two-step process. Also, 0 K dissociation enthalpies of $BOX_2^{\bullet}$ into $I^{\bullet}$ and OBI were found between + 4.1 kJ/mol and + 14.4 kJ/mol dependent on the isomer, indicating that any $BOX_2^{\bullet}$ does not survive the CID process.

3.2.2. Loss of $Y_2H^{\bullet}$

Loss of $Y_2H^{\bullet}$ (blue in Table 1) - with Y representing a boron-bound halogen substituent in the precursor ion is another fragmentation pathway that likely involves multiple steps. Indeed, although previously examined in PES experiments, [44–46] molecules of the type Y-H-$Y^{\bullet}$ (Y = halogen atom) are fairly unstable and have received attention in theoretical chemistry as vibrationally-bound species. [47,48] Fragments formed by a neutral loss of $Y_2H^{\bullet}$ were highly abundant species in CID spectra of several precursor ions (see ions 4, 5, 6, and 12 in Table 1). Both boron-bound hydrogens and hydrogens from the functional groups contribute to this neutral loss. In the case of carborate anions, we noticed that hydrogens from the functional groups (e.g. NH_2) are preferentially incorporated in Y_2H in comparison to boron-bound hydrogens. Fig. 4d demonstrates this for [1-D_2N-2-F-*closo*-1-$CB_{11}I_7H_2(O_2)$]$^{-\bullet}$, which was generated from [1-H_2N-2-F-*closo*-1-$CB_{11}I_8H_2$]$^{-}$ and deuterated methanol. Although the precursor ion contains equal numbers of hydrogen and deuterium atoms, loss of $I_2D^{\bullet}$ is substantially more abundant than loss of $I_2H^{\bullet}$, indicating that the ND_2 ligand is the main contributor of the hydrogen atoms involved in this fragmentation pathway and no significant H/D scrambling is observed.

3.2.3. Loss of $BO_2^{\bullet}$

The loss of $BO_2^{\bullet}$ (green in Table 1) was observed for CB_{11} ions but not for B_{12} ions. After B-O-$O^{\bullet}$ is cleaved, rearrangement into O-B-$O^{\bullet}$ is favored by more than 600 kJ/mol. The barrier for this rearrangement was calculated to be around 30 kJ/mol (see transition state in SI4), indicating that this rearrangement likely occurs in CID experiments. The reaction is particularly interesting from a "boron-chemist's point of view", because a highly stable 12-

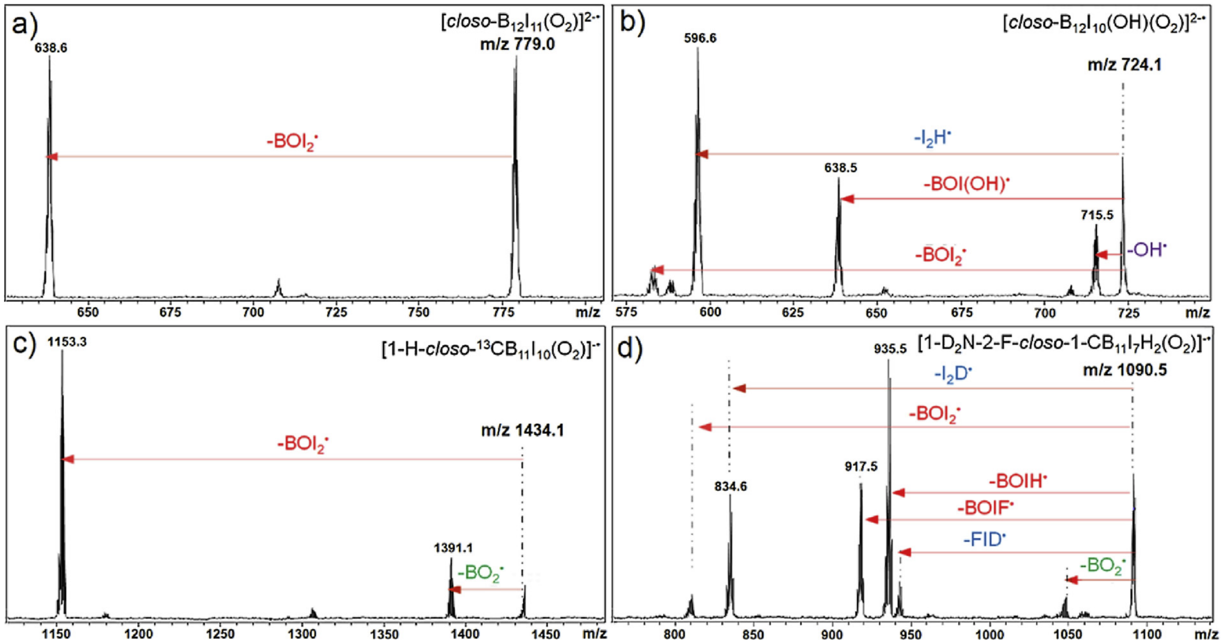

Fig. 4. CID spectra obtained by isolation (width 10 *m/z* units) and fragmentation of a) [*closo*-$B_{12}I_{11}(O_2)$]$^{2-}$, b) [*closo*-$B_{12}I_{10}(OH)(O_2)$]$^{2-}$, c) [1-H-*closo*-1-$^{13}CB_{11}I_{10}(O_2)$]$^{-}$ and d) [1-D_2N-2-F-*closo*-1-$CB_{11}I_7H_2(O_2)$]$^{-}$ formed from the corresponding B_{12} and CB_{11} anions. Isotopic patterns of precursor ions are often strongly distorted in MS/MS spectra. However, product ion patterns are qualitatively preserved as long as a broad isolation window is used in these experiments. In an undistorted pattern of eleven or twelve boron atoms, the most abundant signal is the third isotopologue from the right side of the pattern (compare with Fig. 2). Neutral losses were assigned by examining the difference between the *m/z* of the third isotopic peak from the right side of the unfragmented precursor ion and product ion signals. Additional information regarding neutral loss assignment is provided in section SI2.

Table 1
Summary of neutral losses observed in CID spectra (Fig. 4 and SI2) of highly iodinated B_{12}-O_2 and CB_{11}-O_2 species examined in this study. The corresponding precursor anions are listed in the left column. The colors classify the neutral losses into different categories (see text). "Asterisks" mark the neutral loss, which led to the most abundant product ion, while losses in brackets {} indicate that the corresponding product ions were only observed in very low intensity.

Ion	Precursor B_{12}/ CB_{11} Anions	B_{12}-O_2 / CB_{11}-O_2 Anions[a]	Neutral Losses
1	[*closo*-$B_{12}I_{12}$]$^{2-}$	[*closo*-$B_{12}I_{11}(O_2)$]$^{2-\bullet}$	BOI_2*
2	[*closo*-$B_{12}I_{11}Cl$]$^{2-}$	[*closo*-$B_{12}I_{10}Cl(O_2)$]$^{2-\bullet}$	BOI_2*, BOICl
3	[*closo*-$B_{12}I_{11}H$]$^{2-}$	[*closo*-$B_{12}I_{10}H(O_2)$]$^{2-\bullet}$	BOI_2*, {BOIH}, I_2H
4	[*closo*-$B_{12}I_{10}H_2$]$^{2-}$ [b]	[*closo*-$B_{12}I_9H_2(O_2)$]$^{2-\bullet}$	BOI_2, {BOIH}, I_2H*
5	[*closo*-$B_{12}I_{11}(OH)$]$^{2-}$	[*closo*-$B_{12}I_{10}(OH)(O_2)$]$^{2-\bullet}$	{BOI_2}, BOI(OH), I_2H*,OH
6	[*closo*-$B_{12}I_{11}(NH_2)$]$^{2-}$	[*closo*-$B_{12}I_{10}(NH_2)(O_2)$]$^{2-\bullet}$	{BOI_2}, BOI(NH_2), I_2H*, NH_2
7	[1-H-*closo*-$CB_{11}I_{11}$]$^{-}$	[1-H-*closo*-$CB_{11}I_{10}(O_2)$]$^{-\bullet}$	BOI_2*, {I_2H}, BO_2
8	[1,2-H_2-*closo*-1-$CB_{11}I_{10}$]$^{-}$	[1,2-H_2-*closo*-1-$CB_{11}I_9(O_2)$]$^{-\bullet}$	BOI_2*, BOIH, {I_2H}, BO_2
9	[1-H_2N-*closo*-1-$CB_{11}I_{11}$]$^{-}$	[1-H_2N-*closo*-1-$CB_{11}I_{10}(O_2)$]$^{-\bullet}$	BOI_2*, I_2H, BO_2,
10	[1-H-*closo*-1-$CB_{11}I_9H(OH)$]$^{-}$ [b]	[1-H-*closo*-1-$CB_{11}I_8H(OH)(O_2)$]$^{-\bullet}$	BOI_2*, BOI(OH), BOIH, I_2H, BO_2
11	[1-H_2N-2-F-*closo*-1-$CB_{11}I_{10}$]$^{-}$	[1-H_2N-2-F-*closo*-1-$CB_{11}I_9(O_2)$]$^{-\bullet}$	BOI_2, BOFI, I_2H*,IFH, BO_2
12	[1-H_2N-2-F-*closo*-1-$CB_{11}I_9H$]$^{-}$ [b]	[1-H_2N-2-F-*closo*-1-$CB_{11}I_8H(O_2)$]$^{-\bullet}$	BOI_2, BOFI, BOHI, I_2H*, IFH, BO_2
13	[1-H_2N-2-F-*closo*-1-$CB_{11}I_8H_2$]$^{-}$ [b]	[1-H_2N-2-F-*closo*-1-$CB_{11}I_7H_2(O_2)$]$^{-\bullet}$	BOI_2, BOFI, BOHI*, I_2H, IFH, BO_2,
14	[1-H_2N-2-F-*closo*-1-$CB_{11}I_7H_3$]$^{-}$ [b]	[1-H_2N-2-F-*closo*-1-$CB_{11}I_6H_3(O_2)$]$^{-\bullet}$	{BOI_2}, BOHI*, BOFI, {BOFH}, I_2H, IFH, {BO_2}
15	[1-H-12-H_2N-*closo*-1-$CB_{11}I_4H_4Cl_2$]$^{-}$ [b]	[1-H-12-H_2N-$CB_{11}I_3H_4Cl_2(O_2)$]$^{-\bullet}$	{BOI_2}, BOHI*, {BOICl}, {$BOINH_2$}, {BOHCl},{$BOHNH_2$},{BOH_2}, I_2H, {IClH}

a In most cases, the position of the O_2 substituent has not been verified. Thus, most of the anions are mixtures of isomers. *b* Mixture of isomers with an unknown composition.

vertex *closo*-unit of near icosahedral structure is transformed into a significantly less stable 11-vertex *closo*-unit. Only one related reaction, the transformation of [1-H_2N-*closo*-1-$CB_{11}F_{11}$]$^{-}$ into [3-NC-*closo*-$B_{11}F_{10}$]$^{2-}$ [49], was reported in the condensed phase for the {*closo*-CB_{11}} cluster, previously. Following $I^{\bullet}$ loss from the fully substituted precursor, O_2 binds to the vacant boron site of the CB_{11} unit and ruptures one boron out of this stable structural motif. In synthetic boron chemistry, the preparation of 11-vertex *closo*-units is particularly difficult due to the tendency to form much more stable 12- or 10-vertex clusters. [50,51] We were interested in understanding why this elimination of a boron atom from the core was observed only for CB_{11} ions, since the carbon atom was not formally involved in this elimination. DFT investigations were performed to compare the thermochemistry of $BO_2^{\bullet}$ loss from [*closo*-$B_{12}I_{11}(O_2)$]$^{2-\bullet}$ and [1-H-*closo*-1-$CB_{11}I_{10}(O_2)$]$^{-\bullet}$. For [1-H-*closo*-1-$CB_{11}I_{10}(O_2)$]$^{-\bullet}$, three possible isomers must be considered. The O_2 can be bound to a boron atom in an *ortho*, *meta*, or *para* position to the CH group (see Fig. 1). To evaluate if any of these isomers are preferentially formed in our experiments, we first investigated whether the free binding site, which

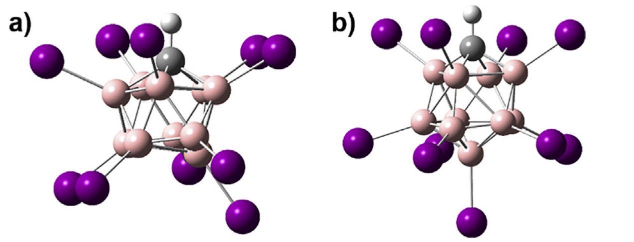

Fig. 5. Optimized structures of the fragment $[n\text{-H-}closo\text{-}n\text{-CB}_{10}I_{10}]^-$ produced by the elimination of $BO_2^{\bullet}$ from a) the *para*-isomer $[1\text{-H-12-}(O_2)\text{-}closo\text{-1-CB}_{11}I_{10}]^{-\bullet}$ or the *meta*-isomer $[1\text{-H-7-}(O_2)\text{-}closo\text{-1-CB}_{11}I_{10}]^{-\bullet}$ and b) from the *ortho*-isomer $[1\text{-H-2-}(O_2)\text{-}closo\text{-1-CB}_{11}I_{10}]^{-\bullet}$. The isomer b) $[2\text{-H-}closo\text{-2-CB}_{10}I_{10}]^-$ is 116.9 kJ/mol more stable than isomer a) $[10\text{-H-}closo\text{-10-CB}_{10}I_{10}]^-$.

subsequently binds O_2, may be formed in all three positions. The thermochemistry of the iodine loss from the precursor $[1\text{-H-}closo\text{-1-CB}_{11}I_{11}]^-$ ion favors the *ortho* position. Loss from *meta* and *para* positions was calculated to be around 7 kJ/mol and 3 kJ/mol higher in energy, respectively (detailed description of the computational methods and results may be found in Section 2.3 and SI5). These comparatively small differences suggest that all three competing fragmentation reactions occur in CID experiments. Based on these results, it is reasonable to assume that in addition to the most stable *ortho* isomer of $[1\text{-H-}closo\text{-CB}_{11}I_{10}(O_2)]^{-\bullet}$, *meta* and *para* isomers of this ion are also produced in CID experiments. Therefore, we calculated the energy associated with abstraction of the $BO_2^{\bullet}$ unit from all three isomers of $[1\text{-H-}closo\text{-CB}_{11}I_{10}(O_2)]^{-\bullet}$ and $[closo\text{-B}_{12}I_{11}(O_2)]^{2-\bullet}$. Although $BO_2^{\bullet}$ loss from both *meta* or *para* isomers of $[1\text{-H-}closo\text{-CB}_{11}I_{10}(O_2)]^{-\bullet}$ produces the same optimized structure of the resulting fragment ion shown in Fig. 5a, $BO_2^{\bullet}$ loss from the *ortho* isomer results in a different, significantly more stable isomer of the fragment ion shown in Fig. 5b. Thermodynamically, the isomer shown in Fig. 5b is roughly 100 kJ/mol more stable than the isomer shown in Fig. 5a, see computational details in SI5. We note that in principle, five different isomers exist for $[n\text{-H-}closo\text{-}n\text{-CB}_{10}I_{10}]^-$ [52], which may interconvert during the CID process [53]. The boron cage structure in Fig. 5b corresponds to the most stable isomer found previously for $[n\text{-H-}closo\text{-}n\text{-CB}_{10}H_{10}]^-$ [53]. DFT calculations also suggest that the formation of this $[2\text{-H-}closo\text{-2-CB}_{10}I_{10}]^-$ isomer by $BO_2^{\bullet}$ loss is roughly 110 kJ/mol more favorable than the formation of $[closo\text{-B}_{11}I_{11}]^{2-\bullet}$ from $[closo\text{-B}_{12}I_{11}(O_2)]^{2-\bullet}$. Subsequent rearrangement of B-O-O$^{\bullet}$ into O-B-O$^{\bullet}$ results in an overall exothermic reaction for $[1\text{-H-2-}(O_2)\text{-}closo\text{-CB}_{11}I_{10}]^{-\bullet}$ (loss from *ortho* position). Meanwhile, the reaction remains endothermic for $[closo\text{-B}_{12}I_{11}(O_2)]^{2-\bullet}$ (see details in SI5). These thermodynamic considerations may be used to rationalize the experimentally observed preferential loss of $BO_2^{\bullet}$ from CB_{11}-O_2 anions. Specifically, it is reasonable to assume that the endothermic loss of $BO_2^{\bullet}$ from B_{12} is associated with a substantially higher barrier than exothermic loss of $BO_2^{\bullet}$ from the *ortho* isomer of CB_{11}-O_2. Future studies will provide detailed theoretical insights into the transition states and possible rearrangement of the $BO_2^{\bullet}$ neutral fragment.

3.2.4. Loss of $OH^{\bullet}$ and $NH_2^{\bullet}$

The radical loss of functional groups, OH and NH_2, was observed exclusively for *closo*-dodecaborate ions, in which the functional groups were directly bound to a boron atom. In contrast, loss of an NH_2 group bonded to the carbon atom in CB_{11}-O_2 ions was not observed.

We note that a low-abundance fragment corresponding to a neutral loss of 31 Da–32 Da was commonly observed, whenever an NH_2 group was bound to carbon, see Fig. 4d and spectra of **9**, **11**, **12**, **13**, **14** in the supporting information. Possible explanations are the loss of NHO or O_2.

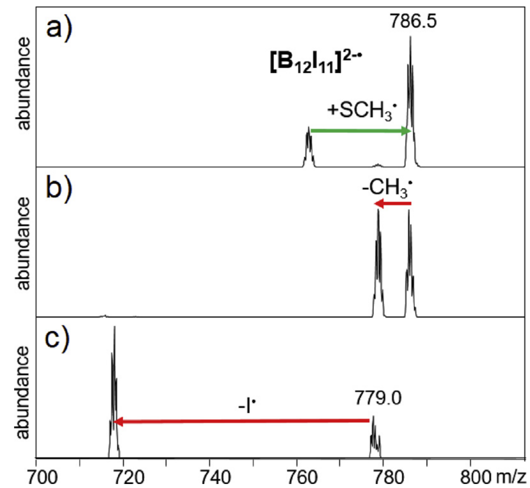

Fig. 6. Mass spectra showing a) the addition of $SCH_3^{\bullet}$ to $[closo\text{-B}_{12}I_{11}]^{2-\bullet}$, b) loss of $CH_3^{\bullet}$ from $[closo\text{-B}_{12}I_{11}(SCH_3)]^{2-}$ and c) $I^{\bullet}$ loss from $[closo\text{-B}_{12}I_{11}S]^{2-\bullet}$. Red arrows indicate fragmentation reactions initiated by CID, green arrows indicate spontaneous reactions.

3.3. Reactions with molecules other than O_2

It is interesting to note that radical *closo*-borate anions of the type $[closo\text{-B}_{12}X_{11}]^{2-\bullet}$ or $[1\text{-H-}closo\text{-1-CB}_{11}X_{10}]^{-\bullet}$ reacted with O_2 but not with H_2O or dinitrogen present in the background of our ion trap. H_2O addition to the even-electron $[closo\text{-B}_{12}I_{11}]^-$ species indicated that water was present in the trap, supporting the observation that the even-electron species, but not the radical anions, displayed reactivity toward H_2O (path 1, Fig. 2). The high selectivity of radical anions like $[closo\text{-B}_{12}I_{11}]^{2-\bullet}$ towards O_2 is thought to be a result of the well-known diradical nature of the triplet O_2. To verify that radicals in general show this reactivity towards $[closo\text{-B}_{12}I_{11}]^{2-\bullet}$, we generated a background atmosphere containing dimethyl disulfide. Recombination of radical ions with $SCH_3^{\bullet}$ is a common reaction under these conditions. [54–57] Addition of $SCH_3^{\bullet}$ to $[closo\text{-B}_{12}I_{11}]^{2-\bullet}$ was observed, yielding the even electron $[closo\text{-B}_{12}I_{11}(SCH_3)]^{2-}$ ion (Fig. 6a). CID of this ion did not result in any boron cage degradation contrary to the degradation observed after the addition of O_2 (chapter 3.2). Instead, fragmentation of the $SCH_3^{\bullet}$ unit via loss of a methyl radical was observed, followed by an iodine loss upon CID of the methyl loss product.

The dominant neutral losses ($BOX_2^{\bullet}$, $Y_2H^{\bullet}$, $BO_2^{\bullet}$) observed in this study for B_{12}-O_2 and CB_{11}-O_2 ions were not observed for other *closo*-borate anions previously. The observed degradation of the boron cage (boron containing neutral losses) of these highly iodinated compounds is particularly interesting in the context of the known gas phase fragmentation pathways of *closo*-borate anions. Boron cage fragmentation has been observed previously for perfluorinated and perchlorinated B_{12} and CB_{11} ions, [18,58] which tend to lose BF_3 and BCl_3 units. However, the presence of multiple iodine atoms usually prevents cage fragmentation. Instead, iodine loss is the preferred channel observed for the highly iodinated $[closo\text{-B}_{12}I_{12}]^{2-}$, $[closo\text{-B}_{12}I_{11}Cl]^{2-}$, $[closo\text{-B}_{12}I_{11}H]^{2-}$, $[closo\text{-B}_{12}I_{11}(OH)]^{2-}$, $[closo\text{-B}_{12}I_{11}(NH_2)]^{2-}$ and $[closo\text{-B}_{12}I_{11}(SCH_3)]^{2-}$ anions. The observation of boron-containing neutral losses $BOX_2^{\bullet}$ and $BO_2^{\bullet}$ from ions like $[closo\text{-B}_{12}I_{11}(O_2)]^{2-\bullet}$ and $[1\text{-H-}closo\text{-1-CB}_{11}I_{10}(O_2)]^{-\bullet}$ is therefore remarkable. It is reasonable to assume that the radical site in the odd-electron $[closo\text{-B}_{12}I_{11}(O_2)]^{2-\bullet}$ species may be responsible for this unusual fragmentation. However, the odd-electron $[B_{12}I_{11}]^{2-\bullet}$ anion does not undergo boron cage degradation, but instead loses $I^{\bullet}$ or I^- in CID experiments.

The boron-oxygen bond, with a bond dissociation energy close to 800 kJ/mol,[59] is one of the strongest chemical bonds. It can be assumed that the presence of this bond may weaken the stability of the boron cage. However, the exclusive loss of iodine from [*closo*-$B_{12}I_{11}(OH)]^{2-}$ does not support this assumption. B_{12}-O_2 and CB_{11}-O_2 ions contain one boron-oxygen bond. The formation of additional B—O bonds is a thermodynamically driven process. A possible explanation for the efficient loss of $BO_2^{\bullet}$ and $BOX_2^{\bullet}$ ions rather than the commonly observed iodine loss may be the formation of an additional boron-oxygen bond in these fragmentation reactions. The likely rearrangement of the $BO_2^{\bullet}$ fragment into O-B-$O^{\bullet}$ (exothermic fragmentation) generates an additional B—O bond. A similar argument may be used for the neutral loss of $BOX_2^{\bullet}$, which generates a boron-oxygen bond in the ion and in the neutral fragment after the reaction. The formation of an additional boron-oxygen bond, which is not possible in fragmentation of non-O_2-containing ions, provides the rationale for the unusual dissociation of B_{12}-O_2 and CB_{11}-O_2 observed in this study.

4. Conclusion

Highly iodinated *closo*-dodecaborate and carba-*closo*-dodecaborate anions fragment by loss of an iodine substituent, leading to formation of radical anions with an unsubstituted boron site. This site spontaneously adds dioxygen (O_2) in ion trap mass spectrometers. PES indicates that the electronic structure of [*closo*-$B_{12}I_{11}(O_2)]^{2-\bullet}$ is very similar to that of [*closo*-$B_{12}I_{12}]^{2-}$. However, CID revealed remarkable differences in fragmentation of highly iodinated B_{12} or CB_{11} anions with and without an O_2 substituent. CID of 15 different O_2-substituted B_{12} and CB_{11} anions (including the substituents H, F, Cl, NH_2 and OH in addition to iodine) was investigated to establish a systematic understanding of the fragmentation pathways of these species. Although highly iodinated clusters usually fragmented by iodine loss, the presence of O_2 in the precursor led to the neutral loss $BOX_2^{\bullet}$, with X representing a boron-bound substituent. Loss of $Y_2H^{\bullet}$ with Y denoting boron-bound halogens was observed when a H atom was present in the precursor and was either bound directly to boron or in a functional group such as NH_2. Loss of $BO_2^{\bullet}$ was observed from CB_{11} but not from B_{12} ions. This difference was explained by the formation of a very stable *ortho*-CB_{10} isomer. Neutral losses of the functional groups, $NH_2^{\bullet}$ and $OH^{\bullet}$, were observed for B_{12} anions. In contrast, for CB_{11} ions these pathways were only observed when the functional group was not bound to the carbon of the cluster. A loss of NHO from CB_{11} ions was observed in low abundance when NH_2 was bound to the carbon atom. The substituent-specific systematic fragmentation patterns may be of analytical value for the identification of functional groups bound to B_{12} and CB_{11} ions with mixed ligand systems.

The selective reactivity of the radical *closo*-borates toward O_2 is traced back to the radical nature of O_2. Recombination of $[B_{12}I_{11}]^{2-\bullet}$ with other radicals is possible, as demonstrated by the reactivity of the cluster toward dimethyl disulfide to abstract $SCH_3^{\bullet}$. However, these ions do not exhibit cage fragmentation. We suggest that the formation of two very strong boron-oxygen bonds is the major driving force for boron- containing neutral losses, which lead to cage fragmentation. Very different CID pathways were observed after recombination of $[B_{12}I_{11}]^{2-\bullet}$ with O_2 and $SCH_3^{\bullet}$. This demonstrates the potential of ion-molecule reactions with radical *closo*-borates to generate a manifold of previously unknown boron compounds using a variety of radical reaction partners. Since we have recently used dodecaborates to demonstrate that gaseous ions may be accumulated via ion soft-landing to prepare condensed-phase layers thicker than 100 nm, [60,61] we propose that fragment ions observed herein may be used in future studies to induce unusual condensed-phase reactions.

Declarations of interest

None.

Acknowledgments

J.W. acknowledges a Feodor Lynen Fellowship from the Alexander von Humboldt Foundation and thanks Dr. John Nash for helpful discussions. M.R. thanks Prof. Simon Grabowsky (University of Bremen) for providing computational resources. The PES work done at Pacific Northwest National Laboratory was supported by the U.S. Department of Energy, Office of Science, Office of Basic Energy Sciences, Division of Chemical Sciences, Geosciences and Biosciences (X.B.W.). Computational research was performed in part using EMSL, a DOE Office of Science User Facility sponsored by the Office of Biological and Environmental Research and located at Pacific Northwest National Laboratory. Battelle operates the Pacific Northwest National Laboratory for the U.S. Department of Energy. H.I.K. acknowledges support from the National Science Foundation NSF (CHE - 1464712). M.F. is grateful to the Deutsche Forschungsgemeinschaft (DFG) for financial support (FI 1628/2-2).

Appendix A. Supplementary data

Supplementary material related to this article can be found, in the online version, at doi:https://doi.org/10.1016/j.ijms.2018.11.005.

References

[1] H. Braunschweig, R.D. Dewhurst, Single, double, triple bonds and chains: the formation of electron-precise B-B bonds, Angew. Chem. Int. Ed. 52 (2013) 3574–3583.
[2] K. Wade, The structural significance of the number of skeletal bonding electron-pairs in carboranes, the higher boranes and borane anions, and various transition-metal carbonyl cluster compounds, J. Chem. Soc. D. (1971) 792–793.
[3] A.J. Welch, The significance and impact of Wade's rules, Chem. Commun. 49 (2013) 3615–3616.
[4] Boron Science: New Technologies and Applications, Taylor & Francis Group, Boca Raton, FL, USA, 2011, CRC Press.
[5] A. Dreuw, L.S. Cederbaum, Multiply charged anions in the gas phase, Chem. Rev. 102 (2002) 181–200.
[6] M.L. McKee, Z.-X. Wang, P. von Ragué Schleyer, Ab Initio Study of the Hypercloso Boron Hydrides B_nH_n and $B_nH_n^-$. Exceptional Stability of Neutral $B_{13}H_{13}$, J. Am. Chem. Soc. 122 (2000) 4781–4793.
[7] H. Zhao, J. Zhou, P. Jena, Stability of $B_{12}(CN)_{12}^{2-}$: Implications for Lithium and Magnesium Ion Batteries, Angew. Chem. Int. Ed. 55 (2016) 3704–3708.
[8] J. Moon, H. Baek, J. Kim, Unusually high stability of $B_{12}(BO)_{12}^{2-}$ achieved by boronyl ligand manipulation: theoretical investigation, Chem. Phys. Lett. 698 (2018) 72–76.
[9] C. Knapp, Weakly Coordinating Anions: Halogenated Borates and Dodecaborates, in: J. Reedijk, K. Poeppelmeier (Eds.), Comprehensive Inorganic Chemistry II, Vol. 1, Elsevier, Amsterdam, 2013, pp. 651–679.
[10] C. Bolli, J. Derendorf, M. Keßler, C. Knapp, H. Scherer, C. Schulz, J. Warneke, Synthesis, Crystal Structure, and Reactivity of the Strong Methylating Agent $Me_2B_{12}Cl_{12}$, Angew. Chem. Int. Ed. 49 (2010) 3536–3538.
[11] D. Stasko, C.A. Reed, Optimizing the Least Nucleophilic Anion. A New, Strong $Methyl^+$ Reagent, J. Am. Chem. Soc. 124 (2002) 1148–1149.
[12] C. Douvris, O.V. Ozerov, Hydrodefluorination of Perfluoroalkyl Groups Using Silylium-Carborane Catalysts, Science 321 (2008) 1188–1190.
[13] J. Warneke, G.-L. Hou, E. Aprà, C. Jenne, Z. Yang, Z. Qin, K. Kowalski, X.-B. Wang, S.S. Xantheas, Electronic Structure and Stability of $[B_{12}X_{12}]^{2-}$ (X = F–At): A Combined Photoelectron Spectroscopic and Theoretical Study, J. Am. Chem. Soc. 139 (2017) 14749–14756.
[14] C. Jenne, M. Keßler, J. Warneke, Protic Anions $[H(B_{12}X_{12})]^-$ (X=F, Cl, Br, I) That Act as Brønsted Acids in the Gas Phase, Chem. Eur. J. 21 (2015) 5887–5891.
[15] J. Warneke, C. Jenne, J. Bernarding, V.A. Azov, M. Plaumann, Evidence for an intrinsic binding force between dodecaborate dianions and receptors with hydrophobic binding pockets, Chem. Commun. 52 (2016) 6300–6303.
[16] W.S. Hopkins, P.J.J. Carr, D. Huang, K.P. Bishop, M. Burt, T.B. McMahon, V. Steinmetz, E. Fillion, Infrared-Driven Charge Transfer in Transition Metal $B_{12}F_{12}$ Clusters, J. Phys. Chem. A 119 (2015) 8469–8475.

[17] M.J. Lecours, R.A. Marta, V. Steinmetz, N. Keddie, E. Fillion, D. O'Hagan, T.B. McMahon, W.S. Hopkins, Interaction of $B_{12}F_{12}^{2-}$ with All-*cis* 1,2,3,4,5,6 Hexafluorocyclohexane in the Gas Phase, J. Phys. Chem. Lett. 8 (2017) 109–113.

[18] J. Warneke, T. Dülcks, C. Knapp, D. Gabel, Collision-induced gas-phase reactions of perhalogenated *closo*-dodecaborate clusters – a comparative study, Phys. Chem. Chem. Phys. 13 (2011) 5712–5721.

[19] M.R. Fagiani, L. Liu Zeonjuk, T.K. Esser, D. Gabel, T. Heine, K.R. Asmis, J. Warneke, Opening of an icosahedral boron framework: A combined infrared spectroscopic and computational study, Chem. Phys. Lett. 625 (2015) 48–52.

[20] P. Farràs, N. Vankova, L.L. Zeonjuk, J. Warneke, T. Dülcks, T. Heine, C. Viñas, F. Teixidor, D. Gabel, From an Icosahedron to a Plane: Flattening Dodecaiodo-dodecaborate by Successive Stripping of Iodine, Chem. Eur. J. 18 (2012) 13208–13212.

[21] M. Rohdenburg, M. Mayer, M. Grellmann, C. Jenne, T. Borrmann, F. Kleemiss, V.A. Azov, K.R. Asmis, S. Grabowsky, J. Warneke, Superelectrophilic Behavior of an Anion Demonstrated by the Spontaneous Binding of Noble Gases to $[B_{12}Cl_{11}]^-$, Angew. Chem. Int. Ed. 56 (2017) 7980–7985.

[22] X.-B. Wang, L.-S. Wang, Development of a low-temperature photoelectron spectroscopy instrument using an electrospray ion source and a cryogenically controlled ion trap, Rev. Sci. Instrum. 79 (2008) 073108.

[23] D. Hanstorp, M. Gustafsson, Determination of the electron affinity of iodine, J. Phys. Chem. B 25 (1992) 1773–1783.

[24] X.-B. Wang, L.-S. Wang, Photodetachment of free hexahalogenometallate doubly charged anions in the gas phase: $[ML_6]^{2-}$, (M=Re, Os, Ir, Pt; L=Cl and Br), J. Chem. Phys. 111 (1999) 4497–4509.

[25] Gaussian 09, Revision D.01, M.J. Frisch, G.W. Trucks, H.B. Schlegel, G.E. Scuseria, M.A. Robb, J.R. Cheeseman, G. Scalmani, V. Barone, G.A. Petersson, H. Nakatsuji, X. Li, M. Caricato, A. Marenich, J. Bloino, B.G. Janesko, R. Gomperts, B. Mennucci, H.P. Hratchian, J.V. Ortiz, A.F. Izmaylov, J.L. Sonnenberg, D. Williams-Young, F. Ding, F. Lipparini, F. Egidi, J. Goings, B. Peng, A. Petrone, T. Henderson, D. Ranasinghe, V.G. Zakrzewski, J. Gao, N. Rega, G. Zheng, W. Liang, M. Hada, M. Ehara, K. Toyota, R. Fukuda, J. Hasegawa, M. Ishida, T. Nakajima, Y. Honda, O. Kitao, H. Nakai, T. Vreven, K. Throssell, J.A. Montgomery, Jr., J.E. Peralta, F. Ogliaro, M. Bearpark, J.J. Heyd, E. Brothers, K.N. Kudin, V.N. Staroverov, T. Keith, R. Kobayashi, J. Normand, K. Raghavachari, A. Rendell, J.C. Burant, S.S. Iyengar, J. Tomasi, M. Cossi, J.M. Millam, M. Klene, C. Adamo, R. Cammi, J.W. Ochterski, R.L. Martin, K. Morokuma, O. Farkas, J.B. Foresman, D.J. Fox, Gaussian, Inc., Wallingford CT, 2016.

[26] A.D. Becke, Density-functional thermochemistry. III. The role of exact exchange, J. Chem. Phys. 98 (1993) 5648–5652.

[27] P.J. Stephens, F.J. Devlin, C.F. Chabalowski, M.J. Frisch, Ab Initio Calculation of Vibrational Absorption and Circular Dichroism Spectra Using Density Functional Force Fields, J. Phys. Chem. 98 (1994) 11623–11627.

[28] M. Valiev, E.J. Bylaska, N. Govind, K. Kowalski, T.P. Straatsma, H.J.J. Van Dam, D. Wang, J. Nieplocha, E. Apra, T.L. Windus, W.A. de Jong, NWChem: A comprehensive and scalable open-source solution for large scale molecular simulations, Comput. Phys. Commun. 181 (2010) 1477–1489.

[29] D. Rappoport, F. Furche, Property-optimized Gaussian basis sets for molecular response calculations, J. Chem. Phys. 133 (2010) 134105.

[30] S. Grimme, J. Antony, S. Ehrlich, H. Krieg, A consistent and accurate ab initio parametrization of density functional dispersion correction (DFT-D) for the 94 elements H-Pu, J. Chem. Phys. 132 (2010) 154104.

[31] S. Grimme, S. Ehrlich, L. Goerigk, Effect of the damping function in dispersion corrected density functional theory, J. Comput. Chem. 32 (2011) 1456–1465.

[32] W.H. Knoth, H.C. Miller, J.C. Sauer, J.H. Balthis, Y.T. Chia, E.L. Muetterties, Chemistry of Boranes. IX. Halogenation of $B_{10}H_{10}^{-2}$ and $B_{12}H_{12}^{-2}$, Inorg. Chem. 3 (1964) 159–167.

[33] J. Holub, S.E. Anwar, T. Jelínek, L. Fojt, Z. Růžičková, V. Šolínová, V. Kašička, D. Gabel, B. Grüner, Polyhalogenated Decaborate and 1-Ammoniododecaborate Ions: An Improved Synthesis with Elemental Halogens, and Physicochemical and Chemical Properties, Eur. J. Inorg. Chem. (2017) 4499–4509.

[34] R.R. Srivastava, D.K. Hamlin, D.S. Wilbur, Synthesis of Highly Iodinated Icosahedral Mono- and Dicarbon Carboranes, J. Org. Chem. 61 (1996) 9041–9044.

[35] M. Finze, J.A.P. Sprenger, 1-Amino-2-fluoromonocarba-*closo*-dodecaborates: K[1-H_2N-2-F-*closo*-1-$CB_{11}H_{10}$] and [Et_4N][1-H_2N-2-F-*closo*-1-$CB_{11}I_{10}$], Z. Anorg. Allg. Chem. 636 (2010) 1538–1542.

[36] S.Z. Konieczka, A. Himmelspach, M. Hailmann, M. Finze, Synthesis, Characterization, and Selected Properties of 7- and 12-Ammoniocarba-*closo*-dodecaboranes, Eur. J. Inorg. Chem. (2013) 134–146.

[37] S.J. Yu, C.L. Holliman, D.L. Rempel, M.L. Gross, The. beta.-distonic ion from the reaction of pyridine radical cation and ethene: a demonstration of high-pressure trapping in Fourier transform mass spectrometry, J. Am. Chem. Soc. 115 (1993) 9676–9682.

[38] R. Li, R.L. Smith, H.I. Kenttämaa, Fluorine Substitution Enhances the Reactivity of Substituted Phenyl Radicals toward Organic Hydrogen Atom Donors, J. Am. Chem. Soc. 118 (1996) 5056–5061.

[39] A. Treu, M. Rittner, D. Kemken, H.-M. Schiebel, P. Spiteller, T. Dülcks, Loss of atomic nitrogen from even-electron ions? A study on benzodiazepines, J. Mass Spectrom. 50 (2015) 978–986.

[40] A.K. Gianotto, B.D.M. Hodges, Pde B. Harrington, A.D. Appelhans, J.E. Olson, G.S. Groenewold, Ion-molecule reactions of gas-phase chromium oxyanions: $Cr_xO_yH_z^-$ + O_2, J. Am. Soc. Mass Spectrom. 14 (2003) 1067–1075.

[41] H. Häkkinen, B. Yoon, U. Landman, X. Li, H.-J. Zhai, L.-S. Wang, On the Electronic and Atomic Structures of Small Au_N^- (N = 4−14) Clusters: A Photoelectron Spectroscopy and Density-Functional Study, J. Phys. Chem. A 107 (2003) 6168–6175.

[42] Z. Qin, G.-L. Hou, Z. Yang, M. Valiev, X.-B. Wang, Negative ion photoelectron spectra of ISO_3^-, $IS_2O_3^-$, and $IS_2O_4^-$ intermediates formed in interfacial reactions of ozone and iodide/sulfite aqueous microdroplets, J. Chem. Phys. 145 (2016) 214310.

[43] C.W. Mathews, The 4465-Å emission spectrum of the BOF_2 molecule, J. Mol. Spectrosc. 19 (1966) 203–223.

[44] R.B. Metz, A. Weaver, S.E. Bradforth, T.N. Kitsopoulos, D.M. Neumark, Probing the transition state with negative ion photodetachment: the chlorine atom + hydrogen chloride and bromine atom + hydrogen bromide reactions, J. Phys. Chem. 94 (1990) 1377–1388.

[45] R.B. Metz, D.M. Neumark, Adiabatic three-dimensional simulations of the IHI^-, $BrHI^-$, and $BrHBr^-$ photoelectron spectra, J. Chem. Phys. 97 (1992) 962–977.

[46] H. Gómez, G. Meloni, J. Madrid, D.M. Neumark, Anion photoelectron spectroscopy of solvated transition state precursors, J. Chem. Phys. 119 (2003) 872–879.

[47] D.C. Clary, J.N.L. Connor, Existence of a bound state for the three-dimensional IHI molecule on a purely repulsive potential energy surface, Chem. Phys. Lett. 94 (1983) 81–84.

[48] D.G. Fleming, J. Manz, K. Sato, T. Takayanagi, Fundamental Change in the Nature of Chemical Bonding by Isotopic Substitution, Angew. Chem. Int. Ed. 53 (2014) 13706–13709.

[49] M. Finze, Carbon Extrusion/Cluster Contraction: Synthesis of the Fluorinated Cyano-*closo*-Undecaborate K_2[3-NC-*closo*-$B_{11}F_{10}$], Angew. Chem. Int. Ed. 46 (2007) 8880–8882.

[50] O. Volkov, P. Paetzold, The chemistry of the undecaborates, J. Organomet. Chem. 680 (2003) 301–311.

[51] F. Klanberg, E.L. Muetterties, Chemistry of Boranes. XXVII. New Polyhedral Borane Anions, $B_9H_9^{2-}$ and $B_{11}H_{11}^{2-}$, Inorg. Chem. 5 (1966) 1955–1960.

[52] P. von Ragué Schleyer, R. Schleyer, K. Najafian, Stability and Three-Dimensional Aromaticity of closo-Monocarbaborane Anions, $CB_{n-1}H_n^-$, and *closo*-Dicarboranes, $C_2B_{n-2}H_n$, Inorg. Chem. 37 (1998) 3454–3470.

[53] R.J. Wiersema, M.F. Hawthorne, Electrochemistry and boron-11 nuclear magnetic resonance spectra of monocarbon carboranes, Inorg. Chem. 12 (1973) 785–788.

[54] K.M. Stirk, J.C. Orlowski, D.T. Leeck, H.I. Kenttamaa, The identification of distonic radical cations on the basis of a reaction with dimethyl disulfide, J. Am. Chem. Soc. 114 (1992) 8604–8606.

[55] J.M. Price, H.I. Kenttämaa, Characterization of Two Chloro-Substituted *m*-Benzyne Isomers: Effect of Substitution on Reaction Efficiencies and Products, J. Phys. Chem. A 107 (2003) 8985–8995.

[56] B.J. Jankiewicz, A. Adeuya, M.J. Yurkovich, N.R. Vinueza, S.J. Gardner, M. Zhou, J.J. Nash, H.I. Kenttämaa, Reactivity of an Aromatic σ,σ,σ-Triradical: The 2,4,6-Tridehydropyridinium Cation, Angew. Chem. Int. Ed. 46 (2007) 9198–9201.

[57] B.J. Jankiewicz, J.N. Reece, N.R. Vinueza, J.J. Nash, H.I. Kenttämaa, Reactivity of the 3,4,5-Tridehydropyridinium Cation—An Aromatic σ,σ,σ-Triradical, Angew. Chem. Int. Ed. 47 (2008) 9860–9865.

[58] A. Himmelspach, J.A.P. Sprenger, J. Warneke, M. Zähres, M. Finze, Mercury (II) Complexes of the Carba-*closo*-dodecaboranyl Ligands [*closo*-1-$CB_{11}X_{11}$]$^{2-}$ (X = H, F, Cl, Br, I), Organometallics 31 (2012) 1566–1577.

[59] T.L. Cottrell, The Strengths of Chemical Bonds, 2d ed, Butterworth, London, 1958, B. de B. Darwent, National Standard Reference Data Series, National Bureau of Standards, no. 31, Washington, 1970.

[60] J. Warneke, M.E. McBriarty, S.L. Riechers, S. China, M.H. Engelhard, E. Aprà, R.P. Young, N.M. Washton, C. Jenne, G.E. Johnson, J. Laskin, Self-organizing layers from complex molecular anions, Nat. Commun. 9 (2018) 1889.

[61] J. Laskin, G.E. Johnson, J. Warneke, V. Prabhakaran, From Isolated Ions to Multilayer Functional Materials Using ion Soft Landing, Angew. Chem. Int. Ed. (2018), http://dx.doi.org/10.1002/anie.201712296.